



BRIEF NOTE

NONLINEAR TORSIONAL DIVERGENCE:
CERTAIN EXACT SOLUTIONS

M. DIMENTBERG

*Mechanical Engineering Department, Worcester Polytechnic Institute
Worcester, MA 01609, U.S.A.*

(Received 26 January 1999 and in revised form 17 May 1999)

Classical analyses of torsional static instability, or divergence, of airfoils or bridge decks in a fluid flow, based on the use of linearized aerodynamic coefficients, lead to a Sturm–Liouville eigenvalue problem — see, e.g., Bisplinghoff & Ashley (1962). Solution to this problem predicts a critical value of the flow speed, such that exceeding this threshold would lead to unlimited growth of twist angles. Most structures are usually designed so as to exclude this instability completely. In some cases, however, such a design requirement may become violated — for example, if some accident happens with the structure involved. Furthermore, it may sometimes be unreasonable or impractical to impose this requirement for civil engineering structures for the case of a possible very strong storm, which has a small but nonzero probability of occurrence. For all such cases the nonlinear analysis of the postcritical stress/strain state seems to be crucial for predicting structural reliability. © 1999 Academic Press

THE NONLINEARITY, WHICH MAY RESTRICT THE GROWTH of twist in case of a static instability, may be due to the basic aerodynamic forces involved. It is well known, that the lift force starts to exhibit “softening” nonlinearity, and it may even start to decrease eventually with increasing angle of attack. Thus, an equilibrium postcritical state may be established for a given supercritical flow speed, which leads to the instability of the initial shape of the structure, or buckling. It is this kind of nonlinearity that is accounted for in this paper, with the aim of predicting the (limited) growth of twist rate and twist angle with increasing flow speed beyond its threshold value.

Consider a uniform prismatic bar of length l with fixed ends. If it is exposed to a cross-flow, the resulting aerodynamic lift would provide a torque, which would twist the bar, until balanced by the torque due to elastic stresses in the bar. The condition for balance of these two torques may be written as (Bisplinghoff & Ashley 1962)

$$GJ(d^2\theta/dy^2) + qc_e C_L(\theta) = 0, \quad q = \left(\frac{1}{2}\right)\rho V^2. \quad (1)$$

Here coordinate y is measured along the bar axis, with the coordinates of the (fixed) ends being $y = 0$ and $y = l$, whereas $\theta(y)$ is the twist angle, which is also the angle of attack as long as the latter is assumed to be zero in the untwisted state, GJ is the torsional stiffness of the bar, c_e the offset of the aerodynamic center from the elastic axis of the bar, q the dynamic

pressure (with ρ and V being the fluid density and flow speed, respectively); all these parameters are assumed to be constant along the bar axis, C_L is the lift coefficient. Whilst this coefficient can be used directly for a streamlined cross-section, it should be replaced by an effective vertical force coefficient $C_y = C_L + C_D \sin \alpha$ for a bluff body, to account for a drag force — see, e.g., Blevins (1994). Here C_D and α are the drag coefficient and the angle of attack, respectively. For the resulting vertical force coefficient, the following dependence on the angle of attack will be adopted in this paper:

$$C_y(\theta) = \left[\frac{\partial C_L}{\partial \alpha} + C_D \right]_{\alpha=0} \frac{\tanh k\theta}{k \cosh^2 k\theta}, \tag{2}$$

where $\partial C_L/\partial \alpha$ is the ordinary lift coefficient slope, which corresponds to the linearized lift curve for small angles of attack. The curve given by equation (2) is qualitatively similar to certain typical lift curves for bluff bodies, and may be used to approximate experimentally obtained curves within limited ranges of θ —particularly if the two-term power-series (cubic) approximation is adequate for the second cofactor, which reduces to $\theta[1 - (4/3)(k\theta)^2]$ for small θ . The resulting simple explicit relations between (postcritical) flow speed and twist rate seem to be important for stochastic reliability analyses for cases of a time-variant flow speed.

Denoting

$$\bar{y} = \frac{y}{l}, \quad f(\theta) = \left(\frac{\lambda^2}{k} \right) \left(\frac{\tanh k\theta}{\cosh^2 k\theta} \right), \quad \lambda^2 = \left(\frac{qc_e l^2}{GJ} \right) \left(\frac{\partial C_y}{\partial \alpha} \right)_{\alpha=0}, \tag{3}$$

equation (1), together with the boundary conditions for fixed ends may be rewritten as

$$\theta'' + f(\theta) = 0, \quad \theta(0) = \theta(1) = 0, \tag{4}$$

where primes denote differentiation with the nondimensional coordinate \bar{y} . For vanishingly small k (or θ) this boundary-value problem clearly reduces to a simple linear eigenvalue problem, with the smallest eigenvalue $\lambda = \pi$ providing the critical speed for divergence. In this paper the exact analytical solution is obtained to boundary-value problem (4), based on the following solution for free oscillations (or free waves) as derived by Nesterov (1978):

$$\theta(\bar{y}) = k^{-1} \operatorname{arc\,sinh} \left[\sinh(k\theta^*) \sin \left(\frac{\lambda \bar{y}}{\cosh k\theta^*} \right) \right]. \tag{5}$$

Here θ^* is an arbitrary integration constant; its physical meaning is that it is the amplitude, or maximal magnitude, of solution (5), which is periodic with period

$$T = \left(\frac{2\pi}{\lambda} \right) \cosh k\theta^*. \tag{6}$$

The other integration constant (phase) in solution (5) is zero, as long as the initial condition $\theta(0) = 0$ is satisfied.

In boundary-value problem (4) the response period is given, whereas the response amplitude, or maximal twist angle, should be obtained. This maximum is clearly attained at the midspan, i.e., $\theta^* = \theta(\frac{1}{2})$, and because of symmetry the condition $T/4 = \frac{1}{2}$ may be imposed instead of the second boundary condition in (4). Then, using formula (6), the following expression for response amplitude, or twist angle at midspan, is obtained:

$$\cosh k\theta^* = \frac{\lambda}{\pi}, \quad \theta^* = k^{-1} \operatorname{arc\,cosh} \left(\frac{\lambda}{\pi} \right) = k^{-1} \ln \left(\frac{\lambda}{\pi} + \sqrt{\frac{\lambda^2}{\pi^2} - 1} \right), \tag{7}$$

whereas solution (5) is reduced to

$$\theta(\bar{y}) = k^{-1} \ln [(\sqrt{\lambda^2/\pi^2 - 1}) \sin(\pi\bar{y}) + \sqrt{1 + (\lambda^2/\pi^2 - 1) \sin^2 \pi\bar{y}}] \tag{8}$$

Here a logarithmic representation of the inverse hyperbolic functions was used, together with relations for the hyperbolic functions (Abramowitz & Stegun 1972). Expression (8) describes the postcritical twist of the bar for any given $\lambda > \pi$, i.e., for a given postcritical flow speed. (If this inequality is not satisfied, twist is zero everywhere, which corresponds to the subcritical case with a stable untwisted shape of the bar.)

Differentiating expression (8) yields the twist rate, which is proportional to the shear stresses:

$$\theta' = \frac{\left(\frac{\sqrt{\lambda^2 - \pi^2}}{k}\right) \cos(\pi\bar{y})}{\sqrt{1 + \left(\frac{\lambda^2}{\pi^2} - 1\right) \sin^2(\pi\bar{y})}}, \tag{9a}$$

so that

$$\theta'_{\max} = \theta'(0) = k^{-1} \sqrt{\lambda^2 - \pi^2}. \tag{9b}$$

It may be of some interest to compare these exact results with those obtained by a simple harmonic balance, or Galerkin-type approximation. A simple half-wave of sinusoid may be used as a trial function, or assumed mode, so that a solution is sought of the form

$$\theta(\bar{y}) = \theta^* \sin(\pi\bar{y}), \tag{10a}$$

and thus

$$\theta'(\bar{y}) = \pi\theta^* \cos(\pi\bar{y}), \tag{10b}$$

which satisfies both boundary conditions. Expression (10a) is substituted into the left-hand side of equation (4) together with its second derivative. Whilst the equation is certainly not satisfied exactly, according to the harmonic balance approximation it may be satisfied in the averaged sense (over a period). Namely, the left-hand side of equation (4) is multiplied by the assumed mode $\sin(\pi\bar{y})$ and integrated within $[0, 1]$. Equating this integral to zero, yields the following equation for the unknown twist amplitude θ^* :

$$\theta^* \left(\frac{\pi}{2}\right) = \int_0^1 f(\theta^* \sin \pi\bar{y}) \sin(\pi\bar{y}) \, d\bar{y}.$$

Using here the expression for f as defined in (3) and retaining the first three terms in the power series expansion for the hyperbolic tangent (Abramowitz & Stegun 1972) yields the following quartic equation for the scaled twist amplitude $A = k\theta^*$:

$$A^4 - \left(\frac{16}{3}\right) A^2 + \left(\frac{16}{3}\right)(1 - \pi^2/\lambda^2), \tag{11a}$$

so that

$$A^2 = \left(\frac{8}{3}\right) [1 - \sqrt{1 - \left(\frac{3}{4}\right)(1 - \pi^2/\lambda^2)}]; \tag{11b}$$

(using, properly, the negative sign for solution of the quadratic equation for A^2 yields $A \rightarrow 0$ with $\lambda \rightarrow \pi + 0$.)

In Figure 1(a) the approximate solution (11b) is compared with the exact results, calculated from the last expression (7). Similarly, in Figure 1(b) the approximate, scaled maximal twist rate $k\theta'_{\max} = \pi A$ [see expression (10b)] is compared with the exact one as

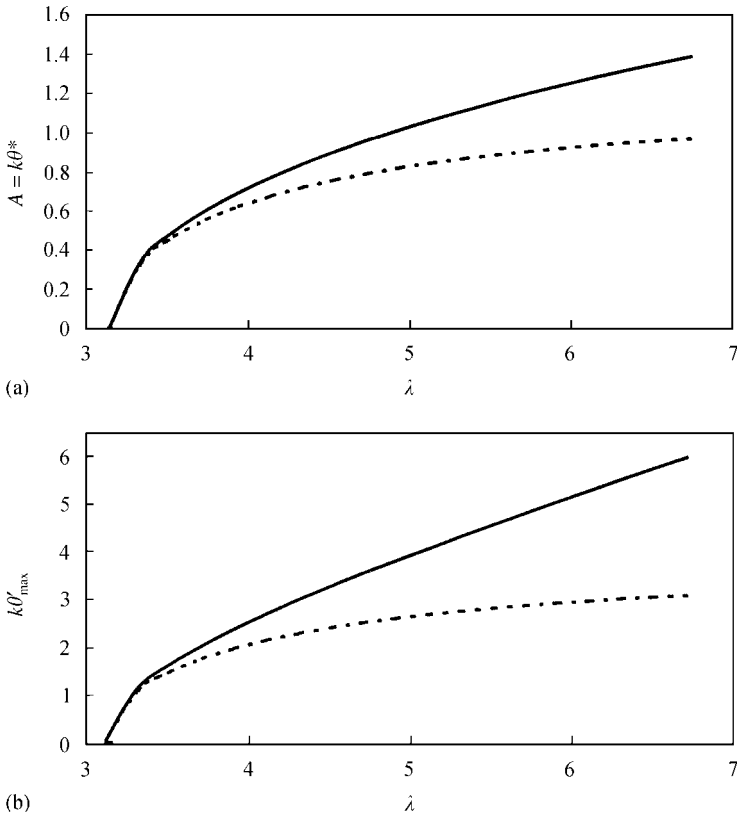


Figure 1. (a) Scaled maximal twist angle $A = k\theta^*$ and (b) scaled maximal twist rate $k\theta'_{\max}$, as functions of the flow speed parameter λ within the postcritical state. Solid lines represent exact results; dashed lines are results based on the harmonic-balance approximation (11b).

governed by expression (9b). Both sets of curves illustrate the increasing inaccuracy of the approximate approach with increasing λ (moving deeper into the domain of instability increases the apparent nonlinearity). Furthermore, as could be expected, inaccuracy in twist rate is larger than in twist angle. On the other hand, with $\lambda/\pi \rightarrow 1 + 0$ equation (7) for A and the approximate expression (11b) both are clearly reduced to

$$A = \sqrt{1 - \left(\frac{\pi}{\lambda}\right)^2}, \tag{12}$$

whereas equation (9) reduces to the corresponding approximate formula for πA . The simple formula (12) may be regarded then as a “universal” law for postcritical behavior for small excess flow speeds, valid for any arbitrary and smooth $f(\theta)$ —up to a constant factor as defined by the coefficient of the cubic term in its power series expansion.

The above solution may be used for the case where only a symmetric middle part of the bar is exposed to the flow. The length of this part is denoted by l , and that of the whole bar by L (see Figure 2). Within the unexposed part of the bar the twist-angle distribution is linear, resulting in the following matching condition at point C, i.e., at the left end of the exposed part:

$$\theta = \left[\frac{(L - l)}{2} \right] \left(\frac{d\theta}{dy} \right) \quad \text{at} \quad y = (L - l)/2, \tag{13}$$

where the coordinate y has its origin at the fixed end of the bar.

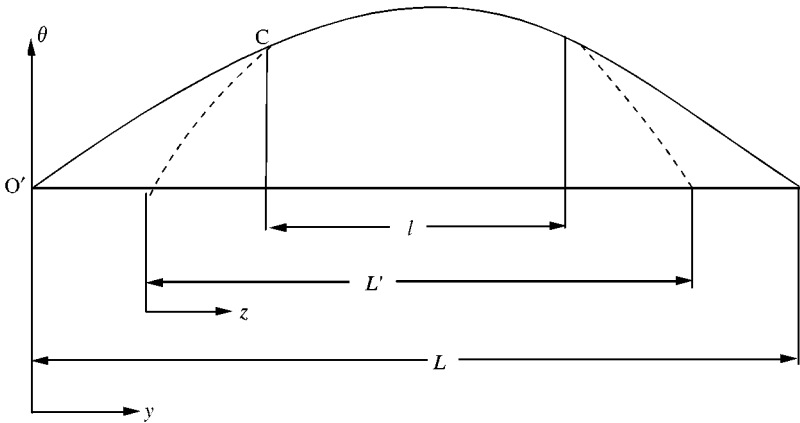


Figure 2. Schematic distribution of twist angle in a bar of length L in case where only its part of length l is exposed to a fluid flow (solid line). An extension of the middle part, which corresponds to a fully exposed bar of length L' , is also shown (dashed lines).

To solve the resulting problem for a fully exposed bar of length l with elastically supported ends, consider it as a part of an auxiliary extended fully exposed bar with fixed ends. The extensions, shown in the Figure 2 by dashed lines, are generated according to the matching condition (13). This condition is used to calculate the resulting length L' of the auxiliary fully exposed bar. A new coordinate along the bar axis is introduced as $z = y - (L - L')/2$, with its origin O' at the left (fixed) end of the fully exposed bar. Introducing the new nondimensional coordinate as $\bar{z} = z/L' = z/\mu l$, where $\mu = L'/l$, we may directly apply equations (7)–(9) to the extended bar, by replacing \bar{y} by \bar{z} and λ by $\tilde{\lambda} = \mu\lambda$ [where $\mu > 1$ and primes denote derivatives with respect to \bar{z} , whereas λ is still defined by the last expression (3)]. The matching condition (13) is imposed at $z = (L' - l)/2L'$, or $\bar{z} = (\frac{1}{2})(1 - 1/\mu)$. Substituting equations (8) and (9), properly adjusted as described, into equation (13) then yields the equation for $\mu = L'/l$:

$$\begin{aligned} & \ln \left\{ \left(\sqrt{(\mu\lambda/\pi)^2 - 1} \right) \sin \left[(\pi/2)(1 - 1/\mu) \right] + \sqrt{1 + [(\mu\lambda/\pi)^2 - 1] \sin^2 \left[(\pi/2)(1 - 1/\mu) \right]} \right\} \\ & = (\pi/2\mu)((L - l)/l) \sqrt{\frac{(\mu\lambda/\pi)^2 - 1}{1 + [(\mu\lambda/\pi)^2 - 1] \sin^2 \left[(\pi/2)(1 - 1/\mu) \right]}} \cos \left[(\pi/2)(1 - 1/\mu) \right], \end{aligned} \tag{14}$$

which is valid provided that $\mu\lambda/\pi > 1$ (the condition for divergence). For vanishingly small (positive) values of $(\mu\lambda/\pi)^2 - 1$, equation (14) reduces to

$$\tan \left[(\pi/2)(1 - 1/\mu_0) \right] = (\pi/2\mu_0)(L - l)/l, \tag{15}$$

where subscript zero is used for this special case, which corresponds to the linear eigenvalue problem. Solution of equation (15) leads immediately to the critical flow speed for divergence via formula $\lambda_{crit} = \pi/\mu_0$. Analysis of the postcritical state of the bar is based on numerical solution of equation (14) for μ , for various $\lambda > \lambda_{crit}$ and several assigned values of $(L - l)/l$. The results are presented in Table 1. One can see that the length L' of the corresponding auxiliary fully exposed bar decreases with increasing flow speed, but this decrease is not large, particularly for relatively large exposed parts of the original bar: when $(L - l)/l = 0.5$, the value of μ remains almost the same as obtained from equation (15) for the linear eigenvalue problem.

TABLE 1

Nondimensional length $\mu = L'/l$ of an auxiliary fully exposed bar with fixed ends as a function of the flow speed parameter λ for three different values of $(L - l)/l$. Bold symbols are used for the critical values, which correspond to the instability threshold of the linearized system

$(L - l)/l$ λ	2 μ	1 μ	0.5 μ
1.3065	2.4050	—	—
1.40	2.37930	—	—
1.7207	—	1.8258	—
1.80	2.28931	1.81802	—
2.00	2.25246	1.79943	—
2.1536	—	—	1.4587
2.20	2.21973	1.78220	1.45741
2.50	2.17682	1.75865	1.44931
2.80	2.13983	1.73751	1.44140
3.10	2.10750	1.71845	1.43375
3.40	2.07893	1.70117	1.42639
3.70	2.05342	1.68542	1.41935
4.00	2.03047	1.67100	1.41263
4.30	2.00967	1.65774	1.40622

As long as the length of the auxiliary bar with fixed ends is established, adjusted formulae (7)–(9) may be applied to the central (exposed) part of the original bar. Whilst the maximum of the twist angle is still attained at the midspan, the maximum twist rate is attained at the left end of the exposed zone, or at $\bar{z} = (\frac{1}{2})(1 - 1/\mu)$ in expression (9), as modified by replacing \bar{y} by \bar{z} and λ by $\mu\lambda$. This maximal twist rate is observed within the whole unexposed part of the bar.

The general asymmetric case of a bar with both supports having unequal finite stiffnesses may be handled by using the complete solution

$$k\theta(\bar{y}) = \text{arc sinh} \{ \sinh k\theta^* [B \sin(\lambda\bar{y}/\cosh k\theta^*) + C \cos(\lambda\bar{y}/\cosh k\theta^*)] \}, \quad (16)$$

where B and C are integration constants, satisfying the relation $B^2 + C^2 = 1$.

REFERENCES

- ABRAMOWITZ, M. & STEGUN, I. A. 1972 *Handbook of Mathematical Functions*. New York, Dover.
 BISPLINGHOFF, R. L. & ASHLEY, H. 1962 *Principles of Aeroelasticity*. New York: Dover.
 BLEVINS, R. D. 1994 *Flow-Induced Vibration*. Malabar, FL.: Krieger.
 NESTEROV, S. V. 1978 Examples of nonlinear Klein–Gordon equations, solvable in terms of elementary functions *Proceedings of the Moscow Institute of Power Engineering*, Vol. 357, pp. 68–70 (in Russian).